Check for updates

Geophysical Research Letters

RESEARCH LETTER
10.1029/2023GL104434

Key Points:

- Delft3D modeling quantifies the formative roles of river discharge and tidal amplitude in formation of river- versus tide-dominated deltas
- We simulate for the first time how river-tide interactions lead to channel widening and tidal bar formation in tide-dominated deltas
- Understanding distinct land loss, gain, and formative processes in river- versus tide-dominated deltas are critical for predicting future change

Supporting Information:

Supporting Information may be found in the online version of this article.

Correspondence to:

Z. Xu,
xuzhenhua1003@126.com

Citation:

Xu, Z., & Plink-Björklund, P. (2023). Quantifying formative processes in river- and tide-dominated deltas for accurate prediction of future change. *Geophysical Research Letters*, *50*, e2023GL104434. https://doi.org/10.1029/2023GL104434

Received 5 MAY 2023
Accepted 25 SEP 2023

Author Contributions:

Conceptualization: Zhenhua Xu, Piret Plink-Björklund
Data curation: Zhenhua Xu
Funding acquisition: Zhenhua Xu
Investigation: Zhenhua Xu, Piret Plink-Björklund
Methodology: Zhenhua Xu
Software: Zhenhua Xu
Visualization: Zhenhua Xu
Writing – original draft: Zhenhua Xu
Writing – review & editing: Piret Plink-Björklund

© 2023. The Authors.
This is an open access article under the terms of the Creative Commons Attribution-NonCommercial-NoDerivs License, which permits use and distribution in any medium, provided the original work is properly cited, the use is non-commercial and no modifications or adaptations are made.

Quantifying Formative Processes in River- and Tide-Dominated Deltas for Accurate Prediction of Future Change

Zhenhua Xu[1,2,3] and Piret Plink-Björklund[4]

[1]State Key Laboratory of Petroleum Resources and Prospecting, China University of Petroleum-Beijing, Beijing, China, [2]College of Geosciences, China University of Petroleum-Beijing, Beijing, China, [3]School of Geosciences, Yangtze University, Wuhan, China, [4]Department of Geology and Geological Engineering, Colorado School of Mines, Golden, CO, USA

Abstract Although most deltas are expected to lose land due to climate change and urbanization, tide-dominated deltas have been suggested to gain land. The processes of land change in such deltas are, however, not well understood, and tide-dominated deltas with all their known morphological attributes have not been simulated before. Our Delft3D simulations successfully reproduce tide-dominated delta morphology, and show that tide-dominated deltas with seaward widening and stable channels, elongate tidal bars and a funnel shape form when bidirectional tidal flow occurs along the whole delta. In contrast, tide-influenced but river-dominated deltas protrude from shoreline, and are efficient at gaining land by mouth bar deposition and bifurcations. These differences are a function of tidal-fluvial interactions expressed by month-averaged seaward and lateral velocities. Identification of delta types is thus critical for predicting future land change. We propose morphological metrics to differentiate river- and tide-dominated deltas and test metrics on 40 modern deltas.

Plain Language Summary River deltas build extensive coastal lands that are one of the most economically and ecologically valuable environments on Earth. While many deltas lose land globally due to climate change and urbanization, deltas significantly influenced by tides are suggested to gain land. Here we utilize numerical modeling to explore the relative formative roles of river and tidal flows, and quantify how the land loss and gain processes differ in river- and tide-dominated deltas. We show that deltas where tidal currents dominate throughout the whole delta build land with a low efficiency, because they form narrow elongate bars and seaward widening distributary channels. In contrast, deltas where tidal currents only dominate in seaward reaches are more efficient at gaining land as they build lobate deltas through mouth bar formation. We propose morphological criteria to distinguish river- and tide-dominated deltas, so more accurate predictions of future land loss and gain can be made. We successfully test these criteria on 40 modern deltas, and show that identification of delta types and understanding the relative roles of river and tidal processes are critical for accurately predicting future change in deltas.

1. Introduction

It is hard to overestimate the significance of river deltas, as they are home to over half a billion people, to biodiverse and rich ecosystems, and they are economic and agricultural hotspots (Foufoula-Georgiou et al., 2013; J. Syvitski & Saito, 2007). Deltas are also global change hotspots and highly vulnerable to increasing urbanization and climate change (Giosan et al., 2014; J. Syvitski & Saito, 2007; Vörösmarty et al., 2009). Over 210 million people live in the Ganges-Brahmaputra-Meghna and Mekong deltas alone (Foufoula-Georgiou et al., 2013), both of which are tide-dominated deltas (Nienhuis et al., 2018). Tide-dominated deltas are the largest deltas in the world and provide 53% of water and 48% of sediment discharge to global oceans (Nienhuis et al., 2020). Although most deltas are expected to lose land, tide-dominated deltas have been suggested to gain land, and tidal influence is expected to increase in future deltas (Nienhuis et al., 2020). This raises questions about how the land loss and gain processes, and the sensitivity to global change differ in tide-dominated deltas.

River delta growth and morphology result from an intricate balance between erosion and deposition from river, tide and wave processes (Galloway, 1975; Orton & Reading, 1993). The evolution of tide-influenced and -dominated deltas, and the land loss and gain processes are primarily a function of river flow and tides (Fagherazzi et al., 2015; Leonardi et al., 2013; Leuven et al., 2019; Nienhuis et al., 2020). The relative roles of these processes are complex and multifaceted, as both have considerable spatiotemporal variations (e.g., Cai et al., 2013; Leonardi

19448007, 2023, 20, Downloaded from https://agupubs.onlinelibrary.wiley.com/doi/10.1029/2023GL104434 by China Universitaet Of Petroleum, Wiley Online Library on [12/10/2023]. See the Terms and Conditions (https://onlinelibrary.wiley.com/terms-and-conditions) on Wiley Online Library for rules of use; OA articles are governed by the applicable Creative Commons License

et al., 2013). River discharge varies with seasons and by human intervention (Elahi et al., 2020; Nienhuis et al., 2020; Nowacki et al., 2019; J. P. M. Syvitski et al., 2009), and tide discharge (tide prism) is affected by estuarine shape and size, tide amplitude and frequency, bed friction, and sea level rise (Du et al., 2018; Gao et al., 2019, 2020; Guo et al., 2016; Khan et al., 2020; Kirwan & Guntenspergen, 2010; Leuven et al., 2018). The actual dynamics of these constantly changing processes are thus difficult to determine (Cao et al., 2020; Goodbred & Saito, 2012; Ji & Zhang, 2020), and numerical modeling hands itself as a useful tool to study the formative roles of river discharge and tides (e.g., Geleynse et al., 2011; Iwantoro et al., 2020, 2022; Leonardi et al., 2013; Sassi et al., 2012). Prior studies have shown the capability of high-resolution physics-based numerical models to accurately resolve the morphology of river deltas under different hydraulic and sedimentary forcings (Edmonds et al., 2021; Geleynse et al., 2011), including models that only consider river and tide processes (Akter et al., 2021; Leonardi et al., 2013; Rossi et al., 2016; Sassi et al., 2012). Models that correctly reproduce deltaic morphology or patterns can be analyzed to understand the processes at work (Edmonds et al., 2021).

Simulations of tidal processes (Iwantoro et al., 2020, 2022; Lerczak & Geyer, 2004; Schramkowski et al., 2010; Zhou et al., 2014), and tide-influenced deltas (Akter et al., 2021; Geleynse et al., 2011; Leonardi et al., 2013; Matsoukis et al., 2023; Rossi et al., 2016) are not uncommon. However, tide-dominated deltas with all their known morphological attributes of seaward widening and stable channels, elongate tidal bars and funnel-shape (e.g., Dalrymple & Choi, 2007; De Swart & Zimmerman, 2009; Goodbred & Saito, 2012) have not been simulated before (see Fagherazzi et al. (2015)). All previous simulations produced tide-influenced deltas with constructional and protruding delta plain with distributary mouth bars (Akter et al., 2021; Geleynse et al., 2011; Iwantoro et al., 2020, 2022; Leonardi et al., 2013; Matsoukis et al., 2023; Rossi et al., 2016).

We simulate 30 tide influenced deltas, that range from tide to river dominated, with Delft3D (v. 4.04.01) (Figure 1 and Figure S3 in Supporting Information S1); and their adjacent off-axis tidal channels that are a generic part of such deltas (see Goodbred and Saito (2012)). What sets our simulations apart from previous tide-influenced delta modeling efforts (e.g., Geleynse et al., 2011; Rossi et al., 2016), is that we allow for erosion along the shoreline. The latter is important because erosion causes land loss, and because erosion is a significant process in forming the morphology of tide-dominated deltas that characteristically do not protrude from shoreline (Figures 2a–2e, and 2g; e.g., Dalrymple & Choi, 2007). Our simulations successfully reproduce tide-dominated delta morphology and we quantify formative processes in tide-dominated versus tide-influenced (river-dominated) deltas, and show that the understanding of the roles of river and tidal processes are essential for accurate prediction of land loss and gain, as well as for understanding the specific effects of global change on deltas. We propose non-dimensional metrics to identify tide-dominated and river-dominated deltas morphologically, and test these metrics on 40 modern deltas.

2. Methods

Delft3D is a high-resolution physics-based numerical model that has been shown to accurately resolve the morphology of coastal systems under different hydraulic and sedimentary forcings (Caldwell & Edmonds, 2014; Edmonds & Slingerland, 2007; Edmonds et al., 2011; Hibma et al., 2004; Wang et al., 2021), including tide-influenced deltas and estuaries (Akter et al., 2021; Baar et al., 2019; Elmilady et al., 2022; Geleynse et al., 2011; Rossi et al., 2016).

We simulate tide-influenced (river-dominated) and tide-dominated deltas, using simulation parameters from the tide-dominated Fly River delta, including dimensions, sediment properties and concentration, monthly river discharge, and tidal range and cyclicity (Canestrelli et al., 2010, 2014) (Text S1.2 in Supporting Information S1). Seasonal discharge variation was also considered, which is an important factor for tide propagation (Elahi et al., 2020). The model domain is 150 km long and 100 km wide, consisting of an initial estuary and adjacent shoreline (Figure 1a). The shoreline is erodible in order to allow for the development of tidal channels and the seaward widening of distributary channels that are characteristic features of tide-dominated deltas (Langbein, 1963; Nienhuis et al., 2018; Wright et al., 1973).

We designed 30 simulations and varied river discharge and tidal amplitude over a range of conditions consistent with natural variations in tide-influenced and -dominated deltas (Canestrelli et al., 2010, 2014; Leonardi et al., 2013) (Figures 1c–1f; see Text S1 in Supporting Information S1 for detailed design and simulations; see Movies S1 and S2 for depositional processes of Run 26 and 30). We focus on the relative roles of river and

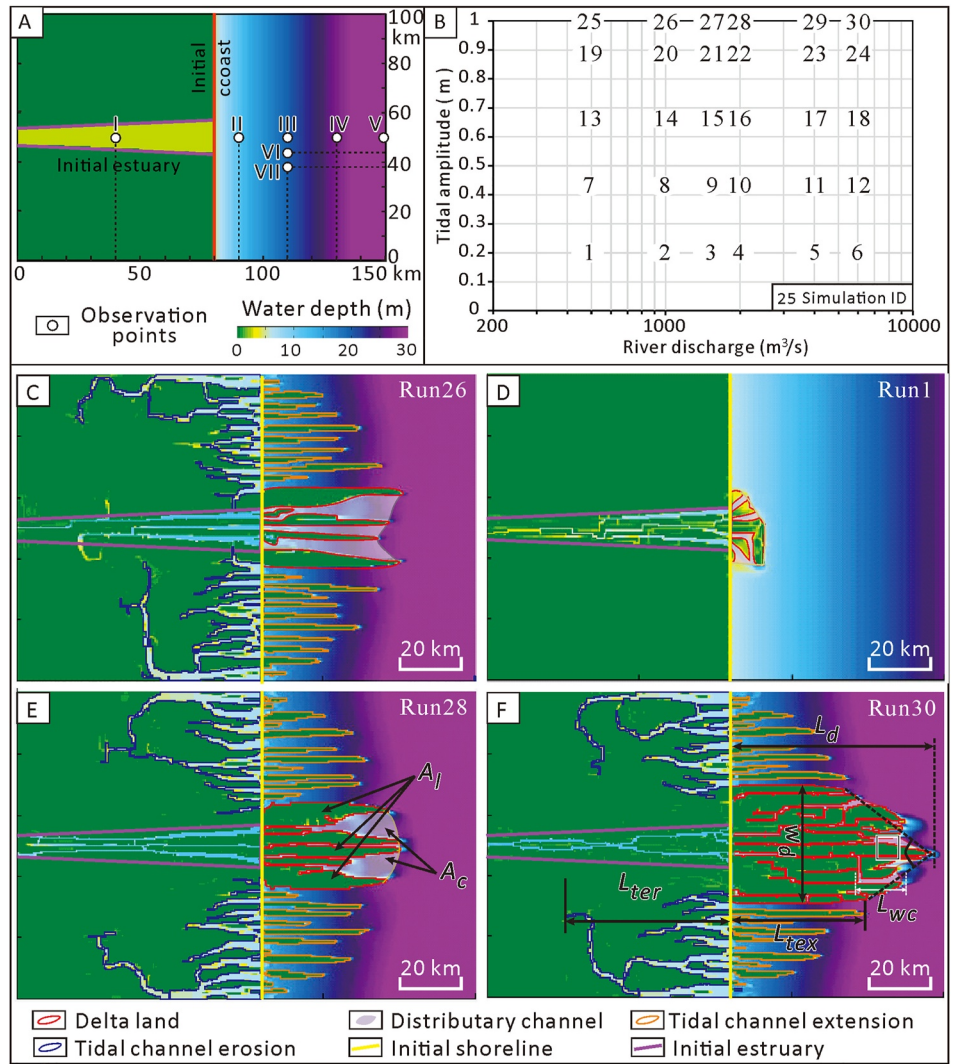

G			
Delta length	L_d	The length of progradation of the axial part of the delta, as measured from the initial shoreline
Delta width	W_d	The width of the delta, measured where the delta is the widest
Shoreline angle	α	The angle of envelope curve of delta front
Nondimensional distributary channel widening length	L_{nwc} (L_{wc}/L_d)	The ratio of the length of the reach where distributary channel widens seaward to the delta length
Distributary channel proportion	A_c/A_d	The ratio of the distributary channel area to the delta area
Land area	A_l	The subaerial area in the delta (excluding the distributary channel area)
Average tidal channel extent	Ave(L_{tex})	The average length of seaward extent of tidal channels, as measured from the initial shoreline
Average tidal channel erosion length	Ave(L_{ter})	The average length of landward incision of tidal channels from the initial shoreline
Tide-dominance ratio	T	The ratio of characteristic mean tidal discharge amplitude (Q_{tide}) to mean annual fluvial discharge (Q_{river}) (Nienhuis et al., 2018)
Delta protrusion degree	P	The relative delta length as compared to the tidal channel seaward extent $(L_d - Max(L_{tex}))/L_d$

Figure 1. (a) Simulation domain, (b) design, and (c–f) four examples of modeled tide-influenced deltas. Runs 26 ($T = 3.8$) and 28 ($T = 1.9$) are examples of tide-dominated deltas and Runs 1 ($T = 0.02$) and 30 ($T = 0.63$) of river-dominated deltas. T is Nienhuis et al. (2018) tide-dominance ratio. I–VII indicate locations of observation points in Figure 4. (e, f) illustrate the morphometric measurement methods defined in panel (g).

19448007, 2023, 20, Downloaded from https://agupubs.onlinelibrary.wiley.com/doi/10.1029/2023GL104434 by China Universitaet Of Petroleum, Wiley Online Library on [12/10/2023]. See the Terms and Conditions (https://onlinelibrary.wiley.com/terms-and-conditions) on Wiley Online Library for rules of use; OA articles are governed by the applicable Creative Commons License

10.1029/2023GL104434

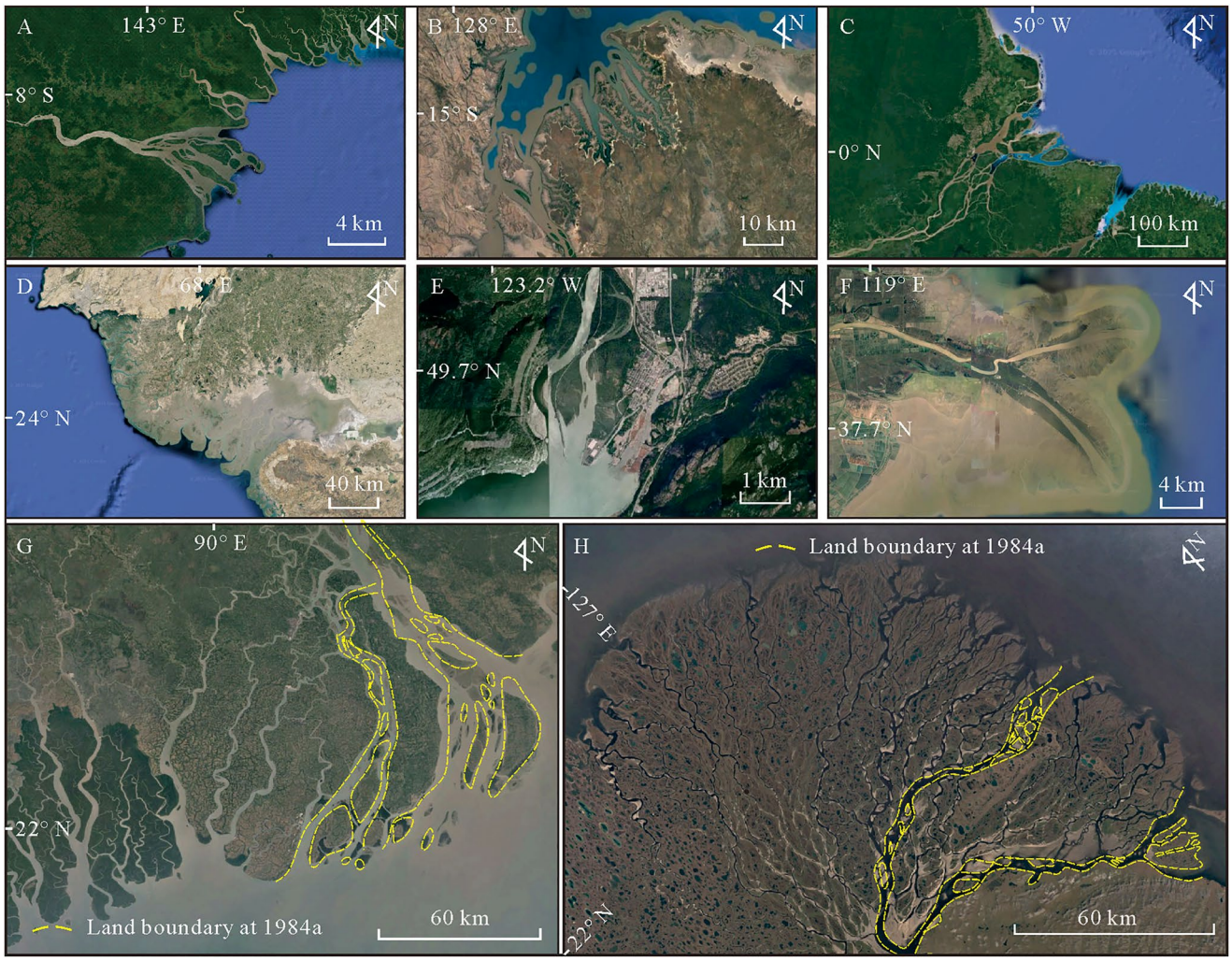

Figure 2. Satellite maps of modern tide-influenced and -dominated deltas. (a) Fly River Delta; (b) Ord River Delta; (c) Amazon River Delta; (d) Indus River Delta; (e) Squamish River Delta; (f) Huanghe Delta; (g) Ganges River Delta; and (h) Lena River Delta. The 1984 shoreline (yellow line) in the Ganges and Lena River Deltas was traced using Google Earth.

tidal processes, and omit waves and sedimentary forcings in order to avoid overcomplication (see also Akter et al. (2021), Leonardi et al. (2013), and Sassi et al. (2012)).

We conducted a numerical validation for jet spread according to theory (Özsoy & Ünlüata, 1982) that has been applied in previous studies (Leonardi et al., 2013; Nardin et al., 2013) (see Text S2 in Supporting Information S1). We tested the robustness of the model by 46 expanding simulations (Text S3 in Supporting Information S1). Changing these parameters indeed modified some morphological characteristics of simulated deltas, but they had minimal effects (<10%) on the morphological recognition criteria that are of interest in this study (Figure S8 in Supporting Information S1), similar to sediment supply variations (Figure S9 in Supporting Information S1). Sediment supply changes concomitantly with discharge.

The simulated deltas evolved by processes similar to those observed in field studies, including delta progradation and mouth bar growth (DuMars, 2002), bi-directional flows (Canestrelli et al., 2010; Olariu et al., 2012), channel widening and elongation (Nienhuis et al., 2018; Plink-Björklund, 2012; Sassi et al., 2012), and tidal shoreline erosion (Goodbred & Saito, 2012; Plink-Björklund, 2012). We further tested whether the model correctly reproduces deltaic morphology, by measuring the morphological criteria in 40 modern tide- and river-dominated deltas (Figure S7 and Table S3 in Supporting Information S1).

19448007, 2023, 20, Downloaded from https://agupubs.onlinelibrary.wiley.com/doi/10.1029/2023GL104434 by China Universitaet Of Petroleum, Wiley Online Library on [12/10/2023]. See the Terms and Conditions (https://onlinelibrary.wiley.com/terms-and-conditions) on Wiley Online Library for rules of use; OA articles are governed by the applicable Creative Commons License

19448007, 2023, 20, Downloaded from https://agupubs.onlinelibrary.wiley.com/doi/10.1029/2023GL104434 by China Universitaet Of Petroleum, Wiley Online Library on [12/10/2023]. See the Terms and Conditions (https://onlinelibrary.wiley.com/terms-and-conditions) on Wiley Online Library for rules of use; OA articles are governed by the applicable Creative Commons License

3. Metrics

Nienhuis et al. (2018) quantify tide-dominated deltas using a tide-dominance ratio, T, which is the ratio of characteristic mean tidal discharge amplitude (Q_{tide}) to mean annual fluvial discharge (Q_{river}). If $T > 1$ the delta is tide-dominated, and if $T < 1$ the delta is river-dominated. We calculate this criterion to initially define river- (tide-influenced) and tide-dominated deltas (Table S1 in Supporting Information S1). Tides are present in all our simulations, and all the simulated deltas are tide influenced.

Although the effect of tides on deltas is complex, seaward distributary channel widening has been suggested as a first-order effect (Langbein, 1963; Nienhuis et al., 2018; Wright et al., 1973). A relative increase in tidal amplitude has been suggested to elongate distributary channels (Geleynse et al., 2011; Hoekstra, 1993; Plink-Björklund, 2012; Sassi et al., 2012), increase the shoreline rugosity (Geleynse et al., 2011; Orton & Reading, 1993; Rossi et al., 2016) and affect the number of distributary channels (Nienhuis et al., 2018). Based on these previous studies and the morphological differences observed in our simulations, we adopted a range of metrics to quantify the relative effects of river discharge and tides on delta morphology (Figures 1e–1g).

In order to study the processes responsible for the characteristic morphological attributes, we quantify the formative roles of river and tidal flow. River flow is unidirectional and seaward directed, tidal flow is bidirectional. We quantify the river and tidal flow interactions, and how they change along the delta axis by extracting month-averaged seaward flow velocities V_{ms} as vectors, where positive value is seaward and negative value landward flow. V_{ms} close to zero indicates bidirectional current, and a positive and high V_{ms} indicates river outflow dominance. In addition to bidirectionality, the river and tide interaction-induced lateral flow is considered a first-order control, leading to baroclinic pressure gradient force in tide-influenced systems (Geyer et al., 1998; Huijts et al., 2006; Lerczak & Geyer, 2004). We calculate these lateral flow velocities V_{ml} as a scalar (along N-S direction in simulations) at different observation points (Figure 1a). We calculate V_{ms} and V_{ml} in fixed observation points I-VII (Figure 1a), over which the deltas prograde over time. We then use V_{ms} and V_{ml} to define fluvial, interaction, and tidal regions.

4. Results

4.1. Axial Delta Morphology

In tide-dominated deltas ($T > 1$), delta length scales to the length of tidal bars and tide-influenced channels, and increases with increasing tidal amplitude, rather than river discharge (Figure 3a). In river-dominated deltas ($T < 1$), delta length is determined by river-dominated distributary channel length, which increases with river discharge and is independent of the tidal amplitude. Therefore, delta length seems threshold-driven and controlled by the dominant process. Delta width increases in both delta types when river discharge increases (Figure 3b), and shoreline angle increases with an increase in tidal amplitude and a decrease in river discharge (Figure 3c).

Distributary channels widen seaward in all tide-influenced deltas (Figure S3 in Supporting Information S1). High river discharge and low tidal amplitude reduce the length of the widening channel reaches, and vice versa (Figure 3d). In tide-dominated deltas ($T > 1$), distributary channels widen seaward throughout the whole delta domain (nondimensional distributary channel widening length $L_{nwc} = 1$). In river-dominated deltas ($T < 1$), $L_{nwc} < 1$, and it scales with both river discharge and tidal amplitude. When T is <0.5, L_{nwc} has a value of ca 0.3, indicating that distributary channel widening is limited to the seaward one-third of these deltas. Distributary channel proportion is influenced by river discharge and tidal amplitude, but river discharge is the primary controlling factor (Figure 3e). When river discharge is >1,500 m^3/s, distributary channel proportion is <0.35 (Figure 3e). Consequently, the land area increases with a high gradient when river discharge is more than 1,500 m^3/s in river-dominated deltas, and it increases with a low gradient with increasing tidal amplitude in tide-dominated deltas (Figure 3f).

4.2. Tidal Channel Morphology

Tidal channels characteristically occur in and adjacent to the natural tide-influenced deltas (Goodbred & Saito, 2012; Hood, 2010). These channels are not connected to the distributary network and only transfer tidal discharges. We successfully model tidal channels and they exhibit higher seaward extent near the axial delta

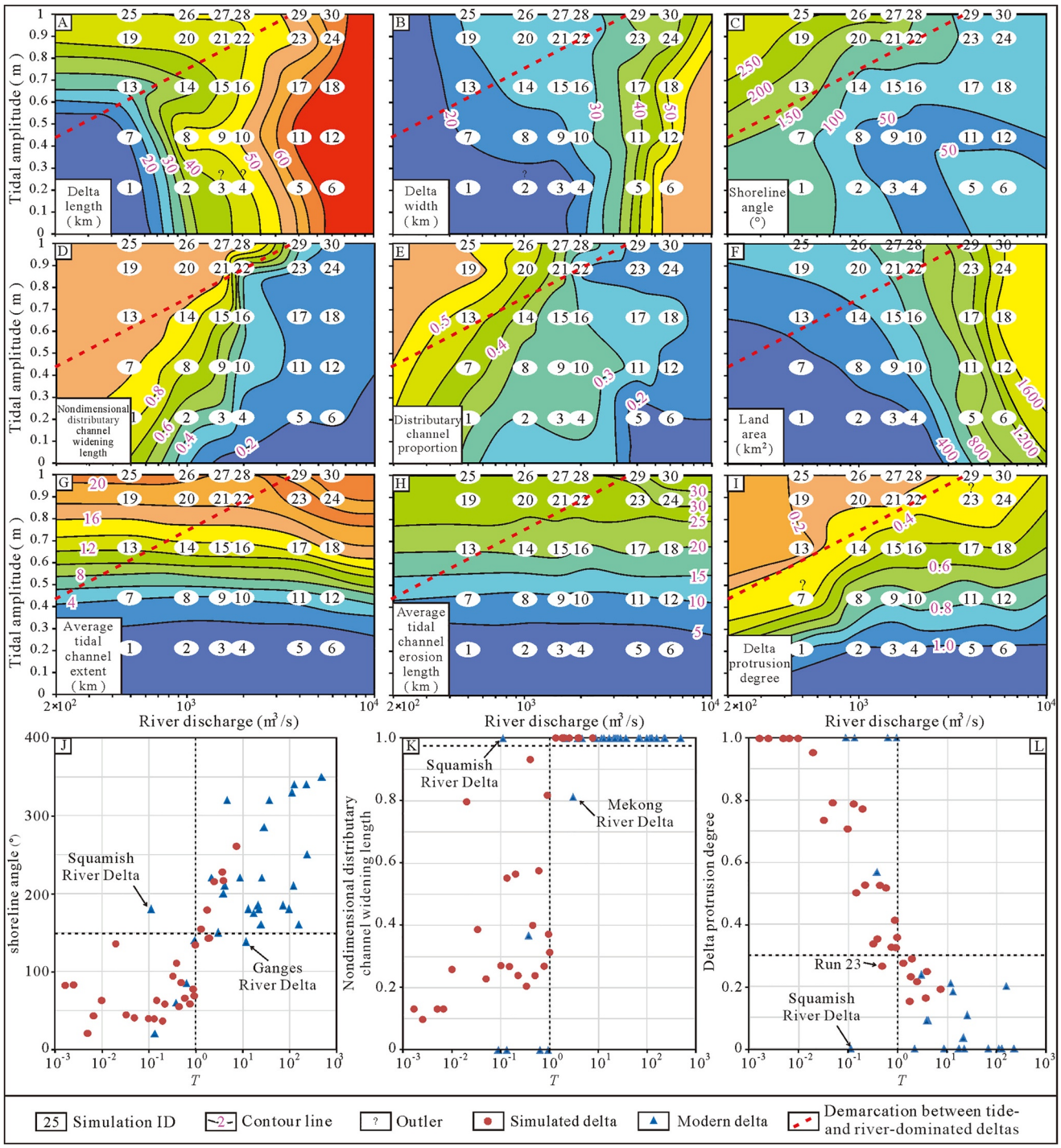

Figure 3. (a–i) Contour maps of nine morphological metrics as functions of river discharge and tidal amplitude. (j–l) Relationships between the Nienhuis et al. (2018) tide dominance ratio (T), and the three here proposed morphological criteria for differentiating tide-dominated and river-dominated deltas. Numbers in the circles indicate locations of simulation data, and the colors from blue to red indicate numerical values from low to high. Red dash lines mark the demarcation between tide- (upper-left) and river-dominated deltas (lower-right), as determined by T value.

and higher landward erosion length further away from the axial delta (Figure 1). Despite this difference, both the seaward extent and the landward erosion length are primarily controlled by tidal amplitude (Figures 3g and 3h).

19448007, 2023, 20, Downloaded from https://agupubs.onlinelibrary.wiley.com/doi/10.1029/2023GL104434 by China Universitaet Of Petroleum, Wiley Online Library on [12/10/2023]. See the Terms and Conditions (https://onlinelibrary.wiley.com/terms-and-conditions) on Wiley Online Library for rules of use; OA articles are governed by the applicable Creative Commons License

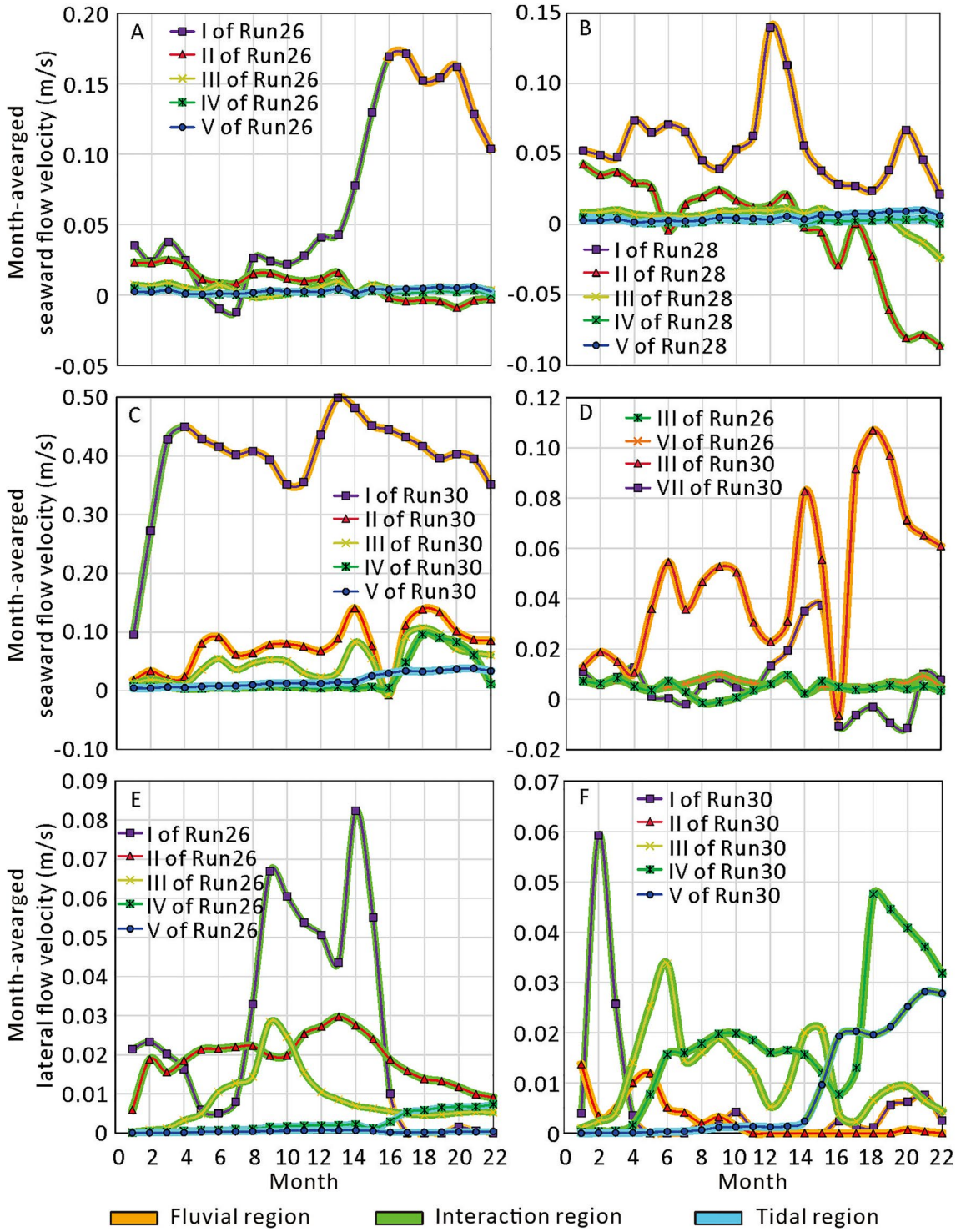

Figure 4. Month-averaged (a–d) seaward (V_{ms}) and (e, f) lateral (V_{ml}) flow velocity variations for tide-dominated (Run 26, 28) and river-dominated (Run 30) deltas at observation points I–VII (see Figure 1a for location).

4.3. River and Tidal Flow Interactions

In tide-dominated deltas, V_{ms} is mostly close to zero, indicating a bidirectional current along the whole delta length, even if T is near to 1 (Run 28) (Figures 4a and 4b). A positive and high V_{ms} that indicates river outflow dominance, only occurs at times in the most upstream section I of tide-dominated deltas (Figures 4a and 4b).

19448007, 2023, 20, Downloaded from https://agupubs.onlinelibrary.wiley.com/doi/10.1029/2023GL104434 by China Universitaet Of Petroleum, Wiley Online Library on [12/10/2023]. See the Terms and Conditions (https://onlinelibrary.wiley.com/terms-and-conditions) on Wiley Online Library for rules of use; OA articles are governed by the applicable Creative Commons License

19448007, 2023, 20, Downloaded from https://agupubs.onlinelibrary.wiley.com/doi/10.1029/2023GL104434 by China Universitaet Of Petroleum, Wiley Online Library on [12/10/2023]. See the Terms and Conditions (https://onlinelibrary.wiley.com/terms-and-conditions) on Wiley Online Library for rules of use; OA articles are governed by the applicable Creative Commons License

In river-dominated deltas, V_{ms} is river outflow dominated in locations I-III, and at times also in location IV (Figure 4c), but is near zero, indicating bidirectional flow in location V (Figure 4c). These differences show that tidal currents dominate along the whole length of tide-dominated deltas, but only in the seaward parts of river-dominated deltas, explaining the observed morphological differences in L_{nwc} (Figure 3d). In tide-dominated deltas V_{ms} remains the same or even slightly increases from delta center to margins (locations II and VI in Run 26, Figure 4d). In river-dominated deltas V_{ms} dramatically decreases from center to margins (locations II and VII in Run 30, Figure 4d).

V_{ml} is relatively high in locations I–III, but near zero in locations IV and V in tide-dominated deltas (Figure 4e). In river-dominated deltas, V_{ml} is relatively high in locations III and IV, and at times also in location V, but it is low in locations I and II (Figure 4f). A temporary high V_{ml} occurs in location I before river flow reaches the initial river mouth.

5. Discussion

5.1. Tide-Versus River-Dominated Delta Morphodynamics

Our results confirm that seaward channel widening is the first-order effect of tides (Langbein, 1963; Nienhuis et al., 2018; Wright et al., 1973). Previous modeling efforts have also suggested that tides in deltas promote more symmetrical and stable bifurcations (Iwantoro et al., 2020, 2022), but also that they increase seaward sediment transport efficiency that results in deeper and more stable distributary channels with less frequent bifurcation and avulsion events (Rossi et al., 2016). Tides have also been suggested to promote distributary channels that are low sinuosity and relatively stable; whereas river processes promote constant channel width, higher sinuosity, and relatively high channel mobility (Gugliotta & Saito, 2019; Gugliotta et al., 2017; Ji & Zhang, 2020; Nienhuis et al., 2018). Tides have further been suggested to increase sediment retention and nutrient and pollutant residence times in deltas thanks to flux convergence and reduced bed shear stress (Glover et al., 2021; McLachlan et al., 2017; Ralston & Geyer, 2017).

Our results show that seaward distributary channel widening, sediment transport efficiency and retention, and mouth bar versus elongate tidal bar formation are a function of tide versus river flow dominance, and their interactions. We observe three regions: fluvial, interaction and tidal regions, defined by V_{ms} and V_{ml}. In fluvial region, V_{ms} is positive and V_{ml} is near zero, indicating the dominance of river flow and weak tidal flow. In this region (locations I-II in river-dominated deltas; Figure 1), we observe mouth bar deposition and consequent distributary channel bifurcations, as expected in river-dominated deltas (Edmonds & Slingerland, 2007) with no channel widening. In tidal region (locations IV-V in tide-dominated and V in river-dominated deltas; Figure 1), V_{ms} and V_{ml} are both near to zero, indicating the dominance of tidal (bidirectional) flow. Here we observe tidal erosion and channel widening (see also Canestrelli et al. (2010) and Schramkowski et al. (2010)). In interaction region (locations I-III in tide-dominated and III-IV in river-dominated deltas; Figure 1), V_{ms} is relatively low and V_{ml} is high, as a result of interaction between riverine and tidal flow.

Distributary channel widening occurs in the tidal and interaction zones in tide-dominated deltas, but only in the tidal zone in river-dominated deltas. This is because, in river-dominated deltas, in the interaction zone, the relatively strong V_{ml} (Figure 4f) and the distinct decrease in V_{ms} from channel center to margins (Figure 4d) promote lateral sediment transport and entrapment at channel margins (see also Fugate et al. (2007), Huijts et al. (2006), and Ralston et al. (2012)). We observe in simulations that sediment is transported downstream and sideways, and finally deposited at the sides of distributary channels (see also Iwantoro et al. (2020)).

In tide-dominated deltas, V_{ms} does not decrease from channel center to margins and promotes channel widening by erosion also in interaction zone. We observe in simulations that V_{ml} rather traps sediments in the central area of the widening channels and forms bars that merge into elongate tidal bars. This prevents bifurcations, and promotes channel stability (see also Iwantoro et al. (2020)), and elongation of tidal bars and distributary channels (see Geleynse et al. (2011)). In tide-dominated deltas, V_{ms} promotes a drawdown of the water surface profile that triggers the development of outward tidal residual currents, which favor channel elongation and tidal-bar progradation (see also Fagherazzi et al. (2015) and Lamb et al. (2012)).

An effect of the differences in V_{ms} and V_{ml} is that in tide-dominated deltas (especially when river discharge is low), distributary channel widening length has a strong positive correlation with tide amplitude increase,

19448007, 2023, 20, Downloaded from https://agupubs.onlinelibrary.wiley.com/doi/10.1029/2023GL104434 by China Universitaet Of Petroleum, Wiley Online Library on [12/10/2023]. See the Terms and Conditions (https://onlinelibrary.wiley.com/terms-and-conditions) on Wiley Online Library for rules of use; OA articles are governed by the applicable Creative Commons License

because increase in tide amplitude promotes erosion. In contrast, in river-dominated deltas (especially when river discharge is high), distributary channel widening length does not covary, or even has a negative correlation with tide amplitude increase, because tides induce more V_{ml} that promotes lateral deposition in river-dominated deltas (Figures 3d and 3e). Consequently, in river-dominated deltas mouth bar formation induces bifurcations and avulsions that form a protruding delta (see also Edmonds and Slingerland (2007) and Olariu and Bhattacharya (2006)), and elongation of distributary channels and mouth bars is restricted to the interaction region, and channel widening to the tidal region. In tide-dominated deltas lateral flow redistributes sediment into elongate tidal bars, and channel widening occurs in interaction and tidal regions, generating a funnel-shaped delta that progrades by distributary channel and tidal bar elongation and forms a delta with a high distributary channel area and stability (see also Dalrymple and Choi (2007), Goodbred and Saito (2012), and Plink-Björklund (2012)).

The importance and dominance of tidal flow in tide-dominated deltas is further shown by that the reworking strength of the tidal currents is similar in the axial delta and the adjacent tidal channels, as the axial deltas exhibit progradation distances similar to the tidal channel seaward extent, resulting in a high shoreline angle and low protrusion length. This further explains why V_{ms} remains the same or even slightly increases from delta center to margins in tide-dominated deltas (Figure 4f).

5.2. Morphological Recognition Criteria

The morphological differences can be utilized as easily used criteria for recognition of tide- and river-dominated deltas. Although we used Nienhuis et al. (2018) criterion T to differentiate tide- and river-dominated deltas, this criterion requires knowledge of river discharge and tidal amplitude, or some other hydrodynamic parameters, which are not always available. Our simulation results suggest that tide-dominated deltas can be identified when the shoreline angle is $\geq 150°$, L_{nwc} is 1, and P is ≤ 0.3.

We tested the effectiveness of these criteria on 40 modern deltas (see Table S3 in Supporting Information S1) that have a diverse morphology (Figure 2) and T values (Figures 3j–3l). In most deltas, T value and the morphological criteria are in agreement (Figures 3j–3l). However, in the Squamish River Delta (Figure 2e) that classifies as a tide-dominated based on the morphological criteria, the T value is only 0.11. We thus show that the morphological criteria are applicable, and help to identify deltas where the T value approach is not possible or the T value is near 1, such as in the Squamish River Delta.

The model validation confirms that the morphological criteria are controlled by the relative strength of river and tidal discharge, and are less influenced by other sedimentary forcings, such as channel and seafloor sand/mud ratio, sediment cohesion, sediment supply, and shoreline erodibility (Text S4 in Supporting Information S1). Thus, although based on simulations with properties of the Fly River delta, these morphological criteria apply globally also in deltas with different sedimentary forcings. These morphological metrics can be calculated using satellite maps, seismic data or even from outcrop data and inter-well analysis.

5.3. Land Building Processes

Our simulations indicate that although distributary channels in tide-dominated deltas are more stable, the land area building is more efficient in river-dominated deltas, even when considering different sediment supply or growth time scenarios (Figure 4 and Figure S9 in Supporting Information S1). Future increase in tidal amplitude would likely result in a larger increase in distributary channel rather than in land area. Climatic and anthropogenic modifications may change the relative strength of river and tidal processes, such as by construction of dams and irrigation, or embankment of tidal intrusion and land reclamation (Hoitink et al., 2017; Nienhuis et al., 2020; J. Syvitski & Saito, 2007; J. P. M. Syvitski et al., 2009). Our results show that tide-dominated deltas will be less sensitive to river discharge changes, such as due to damming or irrigation, because tides dominate the flow along the whole length of the delta. In contrast, river-dominated deltas will be highly sensitive to such changes, but less sensitive to changes in tidal range, such as due to sea-level rise or coastal protection because tidal flow only dominates the seaward portion of the deltas. Furthermore, reduction in river discharge in tide-dominated deltas increases seaward widening distances in distributary channels and elongates tidal bars, whereas it has less influence on delta length. Such changes can be observed in the Ganges River Delta where the 1984–2020 reduction in river discharge resulted in distributary channel widening and elongation of a tidal bar, whereas delta width or length did not change (Figure 2g). In contrast, in river-dominated deltas, changes in river discharge influence

distributary channel widening, as well as delta width and delta length. Such changes can be observed in the Lena delta, where the 1984–2020 increase in river discharge resulted in a decrease in distributary channel widening length and a slight increase in delta length (Figure 2h). In summary, identification of delta types and understanding the relative roles of river and tide processes is critical for accurately predicting future change in deltas.

Data Availability Statement

Data related to this paper can be accessed via Mendeley Data through the following link: https://doi.org/10.17632/ngd7p36jbx.1.

Acknowledgments
The work was financially supported by the National Natural Science Foundation of China (42202178 and 42130813). We thank reviewers Jaap Nienhuis, Douglas Edmonds, and other anonymous reviewers, and the Associate Editor Neil Ganju for constructive reviews that significantly improved the manuscript.

References

Akter, J., Roelvink, D., & van der Wegen, M. (2021). Process-based modeling deriving a long-term sediment budget for the Ganges-Brahmaputra-Meghna Delta, Bangladesh. *Estuarine, Coastal and Shelf Science*, *260*, 107509. https://doi.org/10.1016/j.ecss.2021.107509

Baar, A. W., Albernaz, M. B., van Dijk, W. M., & Kleinhans, M. G. (2019). Critical dependence of morphodynamic models of fluvial and tidal systems on empirical downslope sediment transport. *Nature Communications*, *10*(1), 1–12. https://doi.org/10.1038/s41467-019-12753-x

Cai, H., Savenije, H. G., & Toffolon, M. (2013). Linking the river to the estuary: Influence of river discharge on tidal damping. *Hydrology and Earth System Sciences*, *10*(7), 9191–9238. https://doi.org/10.5194/hessd-10-9191-2013

Caldwell, R. L., & Edmonds, D. A. (2014). The effects of sediment properties on deltaic processes and morphologies: A numerical modeling study. *Journal of Geophysical Research-Earth Surface*, *119*(5), 961–982. https://doi.org/10.1002/2013JF002965

Canestrelli, A., Fagherazzi, S., Defina, A., & Lanzoni, S. (2010). Tidal hydrodynamics and erosional power in the Fly river delta, Papua New Guinea. *Journal of Geophysical Research*, *115*(F4), F04033. https://doi.org/10.1029/2009JF001355

Canestrelli, A., Lanzoni, S., & Fagherazzi, S. (2014). One-dimensional numerical modeling of the long-term morphodynamic evolution of a tidally-dominated estuary: The lower Fly River (Papua New Guinea). *Sedimentary Geology*, *301*, 107–119. https://doi.org/10.1016/j.sedgeo.2013.06.009

Cao, Y., Zhang, W., Zhu, Y., Ji, X., Xu, Y., Wu, Y., & Hoitink, A. J. F. (2020). Impact of trends in river discharge and ocean tides on water level dynamics in the Pearl River Delta. *Coastal Engineering*, *157*, 103634. https://doi.org/10.1016/j.coastaleng.2020.103634

Dalrymple, R. W., & Choi, K. (2007). Morphologic and facies trends through the fluvial–marine transition in tide-dominated depositional systems: A schematic framework for environmental and sequence-stratigraphic interpretation. *Earth-Science Reviews*, *81*(3–4), 135–174. https://doi.org/10.1016/j.earscirev.2006.10.002

De Swart, H. E., & Zimmerman, J. T. F. (2009). Morphodynamics of tidal inlet systems. *Annual Review of Fluid Mechanics*, *41*(1), 203–229. https://doi.org/10.1146/annurev.fluid.010908.165159

Du, J., Shen, J., Zhang, Y. J., Ye, F., Liu, Z., Wang, Z., et al. (2018). Tidal response to sea-level rise in different types of estuaries: The importance of length, bathymetry and geometry. *Geophysical Research Letters*, *45*(1), 227–235. https://doi.org/10.1002/2017GL075963

DuMars, A. J. (2002). *Distributary mouth bar formation and channel bifurcation in the Wax Lake delta, Atchafalaya Bay, Louisiana* (pp. 18–29). Louisiana State University.

Edmonds, D. A., Chadwick, A. J., Lamb, M. P., Lorenzo-Trueba, J., Murray, B. A., Nardin, W., et al. (2021). *Morphodynamic modeling of river-dominated deltas: A review and future perspectives: Treatise on geomorphology* (2nd ed., pp. 1–31). Elsevier Inc. https://doi.org/10.1016/B978-0-12-818234-5.00076-6

Edmonds, D. A., Shaw, J. B., & Mohrig, D. (2011). Topset-dominated deltas: A new model for river delta stratigraphy. *Geology*, *39*(12), 1175–1178. https://doi.org/10.1130/G32358.1

Edmonds, D. A., & Slingerland, R. L. (2007). Mechanics of river mouth bar formation: Implications for the morphodynamics of delta distributary networks. *Journal of Geophysical Research*, *112*(F2), F04038. https://doi.org/10.1029/2006JF000574

Elahi, M. W. E., Jalón-Rojas, I., Wang, X. H., & Ritchie, E. A. (2020). Influence of seasonal river discharge on tidal propagation in the Ganges Brahmaputra-Meghna Delta, Bangladesh. *Journal of Geophysical Research: Oceans*, *125*(11), e2020JC016417. https://doi.org/10.1029/2020JC016417

Elmilady, H., van der Wegen, M., Roelvink, D., & van der Spek, A. (2022). Modeling the morphodynamic response of estuarine intertidal shoals to sea-level rise. *Journal of Geophysical Research: Earth Surface*, *127*, e2021JF006152. https://doi.org/10.1029/2021JF006152

Fagherazzi, S., Edmonds, D. A., Nardin, W., Leonardi, N., Canestrelli, A., Falcini, F., et al. (2015). Dynamics of river mouth deposits. *Reviews of Geophysics*, *53*(3), 642–672. https://doi.org/10.1002/2014RG000451

Foufoula-Georgiou, E., Overeem, I., Saito, Y., Dech, S., Künzer, C., Goodbred, S., et al. (2013). A vision for a coordinated international effort on delta sustainability: In Deltas: Landforms, ecosystems and human activities. In *Proc. of HP1, IAHS-IAPSO-IASPEI assembly* (Vol. 358, pp. 3–11). IAHS Publ.

Fugate, D. C., Friedrichs, C. T., & Sanford, L. P. (2007). Lateral dynamics and associated transport of sediment in the upper reaches of a partially mixed estuary, Chesapeake Bay, USA. *Continental Shelf Research*, *27*(5), 679–698. https://doi.org/10.1016/j.csr.2006.11.012

Galloway, W. E. (1975). *Process framework for describing the morphologic and stratigraphic evolution of deltaic depositional systems*. Deltas: Models for Exploration (pp. 87–98). Houston Geological Society.

Gao, L., Long, H., Tamura, T., Ye, L., Hou, Y., & Shen, J. (2020). Refined chronostratigraphy of a late Quaternary Sedimentary sequence from the Yangtze River delta based on K-feldspar luminescence dating. *Marine Geology*, *427*, 106271. https://doi.org/10.1016/j.margeo.2020.106271

Gao, L., Long, H., Zhang, P., Tamura, T., Feng, W., & Mei, Q. (2019). The sedimentary evolution of Yangtze River delta since MIS3: A new chronology evidence revealed by OSL dating. *Quaternary Geochronology*, *49*, 153–158. https://doi.org/10.1016/j.quageo.2018.03.010

Geleynse, N., Storms, J. E. A., Walstra, D. J. R., Jagers, H. R. A., Wang, Z. B., & Stive, M. J. F. (2011). Controls on river delta formation: Insights from numerical modelling. *Earth and Planetary Science Letters*, *302*(1–2), 217–226. https://doi.org/10.1016/j.epsl.2010.12.013

Geyer, W. R., Signell, R. P., & Kineke, G. C. (1998). Lateral trapping of sediment in a partially mixed estuary. In J. Dronkers & M. B. A. M. Scheffers (Eds.), *Physics of estuaries and coastal seas, PECS 1996* (pp. 115–124). Balkema.

Giosan, L., Syvitski, J., Constantinescu, Ş., & Day, J. (2014). Climate change: Protect the world's deltas. *Nature*, *516*(7529), 31–33. https://doi.org/10.1038/516031a

19448007, 2023, 20, Downloaded from https://agupubs.onlinelibrary.wiley.com/doi/10.1029/2023GL104434 by China Universitaet Of Petroleum, Wiley Online Library on [12/10/2023]. See the Terms and Conditions (https://onlinelibrary.wiley.com/terms-and-conditions) on Wiley Online Library for rules of use; OA articles are governed by the applicable Creative Commons License

Glover, H. E., Ogston, A. S., Fricke, A. T., Nittrouer, C. A., Aung, C., Naing, T., et al. (2021). Connecting sediment retention to distributary channel hydrodynamics and sediment dynamics in a tide-dominated delta: The Ayeyarwady Delta, Myanmar. *Journal of Geophysical Research: Earth Surface*, *126*(3), e2020JF005882. https://doi.org/10.1029/2020JF005882

Goodbred, S. L., & Saito, Y. (2012). Tide-dominated deltas. In R. DavisJr. & R. Dalrymple (Eds.), *Principles of tidal sedimentology* (pp. 129–149). Springer. https://doi.org/10.1007/978-94-007-0123-6_7

Gugliotta, M., & Saito, Y. (2019). Matching trends in channel width, sinuosity, and depth along the fluvial to marine transition zone of tide-dominated river deltas: The need for a revision of depositional and hydraulic models. *Earth-Science Reviews*, *191*, 93–113. https://doi.org/10.1016/j.earscirev.2019.02.002

Gugliotta, M., Saito, Y., Nguyen, V. L., Ta, T. K. O., Nakashima, R., Tamura, T., et al. (2017). Process regime, salinity, morphological, and sedimentary trends along the fluvial to marine transition zone of the mixed-energy Mekong river Delta, Vietnam. In A. S. Ogston, M. A. Allison, J. C. Mullarney, & C. A. Nittrouer (Eds.), *Sediment- and hydro-dynamics of the Mekong delta: From tidal river to continental shelf* (Vol. 147, pp. 7–26). Continental Shelf Research. https://doi.org/10.1016/j.csr.2017.03.001

Guo, L., van der Wegen, M., Wang, Z. B., Roelvink, D., & He, Q. (2016). Exploring the impacts of multiple tidal constituents and varying river flow on long-term, largescale estuarine morphodynamics by means of a 1-d model. *Journal of Geophysical Research: Earth Surface*, *121*(5), 1000–1022. https://doi.org/10.1002/2016JF003821

Hibma, A., Schuttelaars, H. M., & Vriend, H. (2004). Initial formation and long-term evolution of channel–shoal patterns. *Continental Shelf Research*, *24*(15), 1637–1650. https://doi.org/10.1016/j.csr.2004.05.003

Hoekstra, P. (1993). Late Holocene development of a tide-induced elongate delta, the Solo delta, East Java. *Sedimentary Geology*, *83*(3–4), 211–233. https://doi.org/10.1016/0037-0738(93)90014-V

Hoitink, A. J. F., Wang, Z. B., Vermeulen, B., Huismans, Y., & Kästner, K. (2017). Tidal controls on river delta morphology. *Nature Geoscience*, *10*(9), 637–645. https://doi.org/10.1038/ngeo3000

Hood, W. G. (2010). Tidal channel meander formation by depositional rather than erosional processes: Examples from the prograding Skagit River Delta (Washington, USA). *Earth Surface Processes and Landforms*, *35*(3), 319–330. https://doi.org/10.1002/esp.1920

Huijts, K. M. H., Schuttelaars, H. M., de Swart, H. E., & Valle-Levinson, A. (2006). Lateral trapping of sediment in tidal estuaries: An idealized model study. *Journal of Geophysical Research*, *111*(C12), C12016. https://doi.org/10.1029/2006JC003615

Iwantoro, A. P., Van Der Vegt, M., & Kleinhans, M. G. (2020). Morphological evolution of bifurcations in tide-influenced deltas. *Earth Surface Dynamics*, *8*(2), 413–429. https://doi.org/10.5194/esurf-8-413-2020

Iwantoro, A. P., van der Vegt, M., & Kleinhans, M. G. (2022). Stability and asymmetry of tide-influenced river bifurcations. *Journal of Geophysical Research: Earth Surface*, *127*(6), e2021JF006282. https://doi.org/10.1029/2021JF006282

Ji, X., & Zhang, W. (2020). Tidal impacts on downstream hydraulic geometry of a tide-influenced delta. *Ocean Dynamics*, *70*(9), 1239–1252. https://doi.org/10.1007/s10236-020-01391-3

Khan, M. J. U., Durand, F., Testut, L., Krien, Y., & Islam, A. S. (2020). Sea level rise inducing tidal modulation along the coasts of Bengal delta. *Continental Shelf Research*, *211*, 104289. https://doi.org/10.1016/j.csr.2020.104289

Kirwan, M. L., & Guntenspergen, G. R. (2010). Influence of tidal range on the stability of coastal marshland. *Journal of Geophysical Research*, *115*(F2), F02009. https://doi.org/10.1029/2009JF001400

Lamb, M. P., Nittrouer, J. A., Mohrig, D., & Shaw, J. (2012). Backwater and river plume controls on scour upstream of river mouths: Implications for fluvio-deltaic morphodynamics. *Journal of Geophysical Research*, *117*(F1), F01002. https://doi.org/10.1029/2011JF002079

Langbein, W. B. (1963). The hydraulic geometry of a shallow estuary. *Hydrological Sciences Journal*, *8*(3), 84–94. https://doi.org/10.1080/02626666309493340

Leonardi, N., Canestrelli, A., Sun, T., & Fagherazzi, S. (2013). Effect of tides on mouth bar morphology and hydrodynamics. *Journal of Geophysical Research-Oceans*, *118*(9), 4169–4183. https://doi.org/10.1002/jgrc.20302

Lerczak, J. A., & Geyer, W. R. (2004). Modeling the lateral circulation in straight, stratified estuaries. *Journal of Physical Oceanography*, *34*(6), 1410–1428. https://doi.org/10.1175/1520-0485(2004)034<1410:MTLCIS>2.0.CO;2

Leuven, J. R. F. W., de Haas, T., Braat, L., & Kleinhans, M. G. (2018). Topographic forcing of tidal sand bar patterns for irregular estuary planforms. *Earth Surface Processes and Landforms*, *43*(1), 172–186. https://doi.org/10.1002/esp.4166

Leuven, J. R. F. W., Pierik, H. J., Vegt, M. V. D., Bouma, T. J., & Kleinhans, M. G. (2019). Sea-level-rise-induced threats depend on the size of tide-influenced estuaries worldwide. *Nature Climate Change*, *9*(12), 986–992. https://doi.org/10.1038/s41558-019-0608-4

Matsoukis, C., Amoudry, L. O., Bricheno, L., & Leonardi, N. (2023). Numerical investigation of river discharge and tidal variation impact on salinity intrusion in a generic river delta through idealized modelling. *Estuaries and Coasts*, *46*(1), 57–83. https://doi.org/10.1007/s12237-022-01109-2

McLachlan, R. L., Ogston, A. S., & Allison, M. A. (2017). Implications of tidally-varying bed stress and intermittent estuarine stratification on fine-sediment dynamics through the Mekong's tidal river to estuarine reach. *Continental Shelf Research*, *147*, 27–37. https://doi.org/10.1016/j.csr.2017.07.014

Nardin, W., Mariotti, G., Edmonds, D. A., Guercio, R., & Fagherazzi, S. (2013). Growth of river mouth bars in sheltered bays in the presence of frontal waves. *Journal of Geophysical Research: Earth Surface*, *118*(2), 872–886. https://doi.org/10.1002/jgrf.20057

Nienhuis, J. H., Ashton, A. D., Edmonds, D. A., Hoitink, A., Törnqvist, T. E., Rowland, J. C., & Törnqvist, T. E. (2020). Global-scale human impact on delta morphology has led to net land area gain. *Nature*, *577*(7791), 514–518. https://doi.org/10.1038/s41586-019-1905-9

Nienhuis, J. H., Hoitink, A. T., & Törnqvist, T. E. (2018). Future change to tide-influenced deltas. *Geophysical Research Letters*, *45*(8), 3499–3507. https://doi.org/10.1029/2018GL077638

Nowacki, D. J., Ogston, A. S., Nittrouer, C. A., Fricke, A. T., Asp, N. E., & Souza Filho, P. W. M. (2019). Seasonal, tidal, and geomorphic controls on sediment export to Amazon River tidal floodplains. *Earth Surface Processes and Landforms*, *44*(9), 1846–1859. https://doi.org/10.1002/esp.4616

Olariu, C., & Bhattacharya, J. P. (2006). Terminal distributary channels and delta front architecture of river-dominated delta systems. *Journal of Sedimentary Research*, *76*(2), 212–233. https://doi.org/10.2110/jsr.2006.026

Olariu, C., Steel, R. J., Dalrymple, R. W., & Gingras, M. K. (2012). Tidal dunes versus tidal bars: The sedimentological and architectural characteristics of compound dunes in a tidal seaway, the lower Baronia Sandstone (Lower Eocene), Ager Basin, Spain. *Sedimentary Geology*, *279*, 134–155. https://doi.org/10.1016/j.sedgeo.2012.07.018

Orton, G. J., & Reading, H. G. (1993). Variability of deltaic processes in terms of sediment supply, with particular emphasis on grain size. *Sedimentology*, *40*(3), 475–512. https://doi.org/10.1111/j.1365-3091.1993.tb01347.x

Özsoy, E., & Ünlüata, Ü. (1982). Ebb-tidal flow characteristics near inlets. *Estuarine, Coastal and Shelf Science*, *14*(3), 251–263. https://doi.org/10.1016/S0302-3524(82)80015-7

19448007, 2023, 20, Downloaded from https://agupubs.onlinelibrary.wiley.com/doi/10.1029/2023GL104434 by China Universitaet Of Petroleum, Wiley Online Library on [12/10/2023]. See the Terms and Conditions (https://onlinelibrary.wiley.com/terms-and-conditions) on Wiley Online Library for rules of use; OA articles are governed by the applicable Creative Commons License

Plink-Björklund, P. (2012). Effects of tides on deltaic deposition: Causes and response. *Sedimentary Geology*, *279*, 107–133. https://doi.org/10.1016/j.sedgeo.2011.07.006

Ralston, D. K., & Geyer, W. R. (2017). Sediment transport time scales and trapping efficiency in a tidal river. *Journal of Geophysical Research: Earth Surface*, *122*(11), 2042–2063. https://doi.org/10.1002/2017JF004337

Ralston, D. K., Geyer, W. R., & Warner, J. C. (2012). Bathymetric controls on sediment transport in the Hudson River estuary: Lateral asymmetry and frontal trapping. *Journal of Geophysical Research*, *117*(C10), C10013. https://doi.org/10.1029/2012JC008124

Rossi, V. M., Kim, W., López, J. L., Edmonds, D. A., Geleynse, N., Olariu, C., et al. (2016). Impact of tidal currents on delta-channel deepening, stratigraphic architecture, and sediment bypass beyond the shoreline. *Geology*, *44*(11), 927–930. https://doi.org/10.1130/G38334.1

Sassi, M. G., Hoitink, A. J. F., de Brye, B., & Deleersnijder, E. (2012). Downstream hydraulic geometry of a tidally influenced river delta. *Journal of Geophysical Research*, *117*, F04022. https://doi.org/10.1029/2012JF002448

Schramkowski, G. P., de Swart, H. E., & Schuttelaars, H. M. (2010). Effect of bottom stress formulation on modelled flow and turbidity maxima in cross-sections of tide-dominated estuaries. *Ocean Dynamics*, *60*(2), 205–218. https://doi.org/10.1007/s10236-009-0235-0

Syvitski, J., & Saito, Y. (2007). Morphodynamics of deltas under the influence of humans. *Global and Planetary Change*, *57*(3–4), 261–282. https://doi.org/10.1016/j.gloplacha.2006.12.001

Syvitski, J. P. M., Kettner, A. J., Overeem, I., Hutton, E. W. H., Hannon, M. T., Brakenridge, G. R., et al. (2009). Sinking deltas due to human activities. *Nature Geoscience*, *2*(10), 681–686. https://doi.org/10.1038/NGEO629

Vörösmarty, C., Syvitski, J. P. M., Day, J., Paola, C., & Serebin, A. (2009). Battling to save the world's river deltas. *Bulletin of the Atomic Scientists*, *65*(2), 31–43. https://doi.org/10.2968/065002005

Wang, Y., Storms, J. E. A., Martinius, A. W., Karssenberg, D., & Abels, H. A. (2021). Evaluating alluvial stratigraphic response to cyclic and non-cyclic upstream forcing through process-based alluvial architecture modelling. *Basin Research*, *33*(1), 48–65. https://doi.org/10.1111/bre.12454

Wright, L. D., Coleman, J. M., & Thom, B. G. (1973). Processes of channel development in a high-tide-range environment: Cambridge Gulf-Ord River Delta, western Australia. *The Journal of Geology*, *81*(1), 15–41. https://doi.org/10.1086/627805

Zhou, Z., Coco, G., Jimenez, M., Olabarrieta, M., van der Wegen, M., & Townend, I. (2014). Morphodynamics of river-influenced back-barrier tidal basins: The role of landscape and hydrodynamic settings. *Water Resources Research*, *50*(12), 9514–9535. https://doi.org/10.1002/2014WR015891

References From the Supporting Information

Bagnold, R. A. (1966). An approach to the sediment transport problem from general physics. *U. S. Geological Survey Professional Paper*, 422–437.

Bates, C. C. (1953). Rational theory of delta formation. *AAPG Bulletin*, *37*(9), 2119–2162. https://doi.org/10.1306/5CEADD76-16BB-11D7-8645000102C1865D

Battjes, J. A. (1975). Modelling of turbulence in the surf zone. In *Proceedings, symposium on modelling techniques: San Francisco, California, American society of civil engineers* (pp. 1050–1061).

Burpee, A. P., Slingerland, R. L., Edmonds, D. A., Parsons, D., Best, J., Cederberg, J., et al. (2015). Grain-size controls on the morphology and internal geometry of river-dominated deltas. *Journal of Sedimentary Research*, *85*(6), 699–714. https://doi.org/10.2110/jsr.2015.39

Dean, R. G., & Walton, T. L., Jr. (1975). *Sediment transport processes in the vicinity of inlets with special reference to sand trapping: Geology and Engineering* (pp. 129–149). Academic Press.

Dietrich, W. E., Day, G., & Parker, G. (1999). The Fly River, Papua New Guinea: Inferences about river dynamics, floodplain sedimentation and fate of sediment: Varieties of fluvial form (pp. 345–376).

Dissanayake, D. M. P. K., Roelvink, J. A., & Vander Wegen, M. (2009). Modelled channel patterns in a schematized tidal inlet. *Coastal Engineering*, *56*(11–12), 1069–1083. https://doi.org/10.1016/j.coastaleng.2009.08.008

Edmonds, D. A., & Slingerland, R. L. (2010). Significant effect of sediment cohesion on delta morphology. *Nature Geoscience*, *3*(2), 105–109. https://doi.org/10.1038/ngeo730

Hayes, M. O., & Kana, T. W. (1976). Terrigenous clastic depositional environments: Some modern examples. The university of South Carolina, Technical Report 11-CRD, Coastal Research Division (Vol. *131*).

Ikeda, S. (1982). Lateral bed load transport on side slopes. *Journal of the Hydraulics Division*, *108*(11), 1369–1373. https://doi.org/10.1061/JYCEAJ.0005937

Ikeda, S. (1984). Lateral bed-load transport on side slopes-closure. *Journal of Hydraulic Engineering*, *110*(11), 200–203. https://doi.org/10.1061/JYCEAJ.0005937

Koch, F. G., & Flokstra, C. (1980). Bed level computations for curved alluvial channels. *Proc. of the XIX Congress of the IAHR*, *2*, 357–364.

Lesser, G. R., Roelvink, J. V., van Kester, J. T. M., & Stelling, G. S. (2004). Development and validation of a three-dimensional morphological model. *Coastal Engineering*, *51*(8–9), 883–915. https://doi.org/10.1016/j.coastaleng.2004.07.014

Leuven, J. R. F. W., Kleinhans, M. G., Weisscher, S. A. H., & van der Vegt, M. (2016). Tidal sand bar dimensions and shapes in estuaries. *Earth-Science Reviews*, *161*, 204–223. https://doi.org/10.1016/j.earscirev.2016.08.004

Marciano, R., Wang, Z. B., Hibma, A., de Vriend, H. J., & Defina, A. (2005). Modeling of channel patterns in short tidal basins. *Journal of Geophysical Research*, *110*(F1), F01001. https://doi.org/10.1029/2003JF000092

Özsoy, E. (1986). Ebb-tidal jets—A model of suspended sediment and mass-transport at tidal inlets. *Estuarine, Coastal and Shelf Science*, *22*(1), 45–62. https://doi.org/10.1016/0272-7714(86)90023-5

Postma, G. (1990). An analysis of the variation in delta architecture. *Terra Nova*, *2*, 124–130. https://doi.org/10.1111/j.1365-3121.1990.tb00052.x

Tejedor, A., Longjas, A., Caldwell, R., Edmonds, D. A., Zaliapin, I., & Foufoula-Georgiou, E. (2016). Quantifying the signature of sediment composition on the topologic and dynamic complexity of river delta channel networks and inferences toward delta classification. *Geophysical Research Letters*, *43*(7), 3280–3287. https://doi.org/10.1002/2016GL068210

Van Rijn, L. C. (1993). *Principles of sediment transport in rivers, estuaries and coastal seas* (pp. 10–50). Aqua publications.

Wolanski, E., King, B., & Galloway, D. (1997). Salinity intrusion in the fly river estuary, Papua New Guinea. *Journal of Coastal Research*, *13*(4), 983–994. Retrieved from https://www.jstor.org/stable/4298709

Wolinsky, M. A., Edmonds, D. A., Martin, J., & Paola, C. (2010). Delta allometry: Growth laws for river deltas. *Geophysical Research Letters*, *37*(21), L21403. https://doi.org/10.1029/2010GL044592

19448007, 2023, 20, Downloaded from https://agupubs.onlinelibrary.wiley.com/doi/10.1029/2023GL104434 by China Universitaet Of Petroleum, Wiley Online Library on [12/10/2023]. See the Terms and Conditions (https://onlinelibrary.wiley.com/terms-and-conditions) on Wiley Online Library for rules of use; OA articles are governed by the applicable Creative Commons License